Design of a Novel Interleukin-13 Antagonist from Analysis of Informational Structure

A. N. Nekrasov[1]*, L. E. Petrovskaya[1], V. A. Toporova[1], E. A. Kryukova[1], A. V. Rodina[2], E. Yu. Moskaleva[2], and M. P. Kirpichnikov[1]

[1]Shemyakin and Ovchinnikov Institute of Bioorganic Chemistry, Russian Academy of Sciences, ul. Miklukho-Maklaya 16/10, 117997 Moscow, Russia; fax: (495) 330-6983; E-mail: alexei_nekrasov@mail.ru
[2]Moscow Research Institute of Medical Ecology, Department of Health Care, Simferopolsky Bulvar 8, 117638 Moscow, Russia; fax: (496) 113-4827; E-mail: allrodina@yandex.ru

Abstract—Interleukin-13 (IL-13) is one of the cytokines involved in the development of Th2-type immune response. It plays an important role in the pathogenesis of asthma and other allergic diseases. Two deletion forms of IL-13 were constructed on a basis of informational structure analysis and expressed in *E. coli* cells. They were found to differ in ability to stimulate proliferation of TF-1 cell line. Deletion variant 146 (DV146) completely lacks such activity, whereas DV148 provides about 50% of the proliferation stimulation. The simultaneous addition of DV146 with full-length IL-13 suppresses proliferation depending on the concentration of the deletion form. Thus, the designed protein acts as an antagonist of IL-13.

Interleukin-13 (IL-13) is secreted by allergen-activated T-helpers, mastocytes, basophiles, and memory T-cells and affects various cell types (monocytes and macrophages, endothelial and mesothelial cells, B-lymphocytes, etc.) [1-3]. The physiological role of IL-13 is mediated by the interaction with membrane receptors of normal cells that incorporate IL-4Rα and IL-13α1 as subunits [4].

IL-13 regulates the expression of CD23 and MHC (major histocompatibility complex) antigens on naive B-cells and stimulates their proliferation and IgE and IgG4 synthesis [5]. Overexpression of this cytokine accompanies various allergic disorders, in particular asthma [6, 7], thus making the design of artificial IL-13 antagonists a promising trend in bioengineering.

Synthesis of the deletion variants is a natural way to regulate the activity of α-helical cytokines, to which IL-13 belongs [8]. In particular, alternative splicing results in the formation of IL-4 variant IL-4δ2, which is a natural antagonist of this cytokine, i.e. it suppresses IL-4 stimulated T-cell proliferation [9]. The existence of two truncated IL-2 variants (IL-2δ2 and IL-2δ3) was shown experimentally [10]. Both of these variants are concurrent inhibitors of full-length protein suppressing IL-2 binding to its high-affinity receptor.

So far, there is no evidence of natural variants of IL-13 acting as antagonists. This prompted us to design such a form using informational structure analysis and protein engineering techniques. The previously proposed ANIS-method (Analysis of Informational Structure), which relies only upon amino acid sequence of a protein, allows considering protein primary structure as a hierarchy of ELIS (Elements of Informational Structure) [11]. It was shown that it is possible to obtain functionally active truncated forms of proteins by the removal of sequence fragments corresponding to the high-ranking ELIS [12]. The ANIS method was applied to design two IL-13 deletion variants, which were expressed in *E. coli* and studied in experiments with a cell line carrying specific IL-13/IL-4 receptor.

Abbreviations: ANIS, analysis of informational structure; DV, deletion variant; ELIS, elements of informational structure; IDIC, increased degree of information coordination; IDIC-sites, sites with a locally increased degree of information coordination between residues; IL-13, interleukin-13; IPTG, isopropyl-β-D-thiogalactoside; IS, informational structure; IU, informational units; SOE, splice overlap extension.
* To whom correspondence should be addressed.

MATERIALS AND METHODS

Informational structure analysis. Graphic representation of informational structure (IS) (IDIC-diagrams) can be composed using the following algorithm:

− the amino acid sequence of a given protein is encoded as a set of informational units (IU);

− the population profile of the target protein structure by IU is determined;

− sites with a locally increased degree of information coordination between residues (IDIC-sites) are localized within the protein sequence;

− a graphic representation of IS is constructed.

Encoding protein sequences as IU sets. Let $\mathfrak{R}$ be the set of all standard amino acid residues forming primary structure of native protein sequences, i.e. $\mathfrak{R} = \{A, C, D, E, F, G, H, I, K, L, M, N, P, Q, R, S, T, V, W, Y\}$. Then the function $B: \{1...N\} \xrightarrow{B} R$, where N is the number of residues, corresponds to the protein sequence. In the previous work [13], it was shown that in native protein sequences neighboring residues have a high level of coordination with R_{HLCD} distance. On the basis of these data we have proposed the new method of encoding the protein sequences by a set of informational units (IU) $U_i = (B_{i-\delta}, ..., B_{i+\delta})$ each representing a group of ε neighboring residues, where $\varepsilon = 2\delta + 1$ and $\delta = 1, ..., N$. All the informational units of k type (U_k), which are the elements of the set $\mathfrak{I}$, are characterized by the occurrence frequency P_{U_k}. The occurrence frequencies of IUs were used for the analysis of informational structure of studied protein sequences.

Composition of population profile of a protein sequence by IU. The next step in the study of protein informational structure is the composition of the profile $F = \{F(j)\}$ of a protein sequence populated by IU:

$$F(j) = \begin{cases} \sum_{i=j\pm\varepsilon/2} P_{U_i} & if \quad U_j \in \mathfrak{I}, \\ 0 & if \quad U_j \notin \mathfrak{I}, \end{cases} \quad (1)$$

where $j = 1 + \delta ...N - \delta$, $\varepsilon = 2\delta + 1$, and $\mathfrak{I}$ is the set of all possible IU from all non-homologous protein sequences comprising the database of the software WHAT IF [14]. Informational units belong to $\mathfrak{I}$ if 80% of IU forming residues are equal to the elements of $\mathfrak{I}$.

Localization of IDIC-sites in informational structure. IU encoding can be used to compute a value of IU correlation in protein sites having different size. Sites with local high coordination level were called IDIC-sites [11]. To identify the location of IDIC-sites, we introduced a function $f(j')$ for each $j = 1, ..., N$:

$$f(j') = De^{-\frac{(j'-j)^2}{\rho^2}}, \quad (2)$$

determined for all values $j = 1, 2...N$, $\rho = 1 + \delta ... N - \delta$, which complies with the condition:

$$F(j) - f(j') \geqslant 0. \quad (3)$$

The latter condition is the limitation of $f(j')$ function D parameter value.

For each $j = 1, ..., N$, the $D = D(j)$ parameter is chosen to be the maximal of D satisfying condition (3). During the computation, the ρ values were matching interval $\delta < \rho < N - \delta$, where N is the length of the target sequence. At the same time,

$$\omega(j,\rho) = \sum_{j'} D(j)e^{-\frac{(j'-j)^2}{\rho^2}}, \quad (4)$$

can be computed for each $f(j')$ function, where j is the position of IDIC-site in the protein sequence and ρ is the length of the IDIC-site.

Graphic representation of a protein IS (the IDIC-diagram). The IS of a protein can be graphically represented as a surface Γ_ω defined by the function $\omega = \omega(j, \rho)$. A simpler and more convenient representation of IS (the IDIC-diagram) can be constructed by plotting only sites with a locally increased degree of coordination between residues (IDIC-sites) of various length [11]. In this case, instead of the Γ_ω surface only the values of function $\omega(j, \rho)$ remain that comply with the condition of the local maximum existence:

$$\begin{cases} \omega(j,\rho) \geqslant \omega(j+1,\rho) \\ \omega(j,\rho) \geqslant \omega(j-1,\rho). \end{cases} \quad (5)$$

As a result of such approximation the structurally complicated Γ_ω surface is reduced to a limited set of points. By connecting the closest points, which correspond to positions of IDIC-sites of different length ρ, hierarchical graphs of ELIS will be produced. The ELIS is characterized by its position in the protein sequence and in the hierarchy (rank). The rank is equal to the number of node points along the most distant path from lowest-level element to a target node point. The ELIS located at the lowest level of hierarchy is assigned a rank equal to 1.

The WEB-service ANIS-TREES, based on the described method of informational structure analysis, is available at anis.ibch.ru/trees.

Recombinant DNA construction. DNA was cloned according to the standard protocols [15] using XL-1 Blue *E. coli* strain (Stratagene, USA) and enzymes produced by Fermentas (Lithuania). Oligonucleotides were synthesized by Evrogen (Russia). The pHIL13 vector was constructed by cloning the synthetic duplex carrying the hexahistidine tag and the enterokinase cleavage site, HEK51 5′-CGATATGCATCACCATCACCATCACG-GTACCGACGACGACGAC; HEK52 5′-AAGGGTC-CAGTTCCACCATCTACTGCATTGAGAGAGCT; HEK53 5′-ATATGCATCACCATCACCATCACGGTA-

CCGAC; HEK54 5′-GACGACGACAAGGGTCCAGTT-CCACCATCTACTGCATTGAGAG, into the pTrcTREN plasmid [16] by *Cla*I/*Sac*I sites, together with the encoding sequence produced by the artificial splicing of the human IL-13 gene [17].

Deletion variant genes were constructed by the splice overlap extension PCR method (SOE-PCR) using Pfu-polymerase (Fermentas). We first amplified fragments of the human IL-13 gene flanking the deletion with one of the universal primers complementary to the vector and the primer containing the spliced sequence of the deletion variant.

To obtain the fragments of DV146 mutant gene we used primers 13D2BF 5′-*TGGCAGCATGGTA*TACTGT-GCAGCCCTGGAATCCC (the part of the primer corresponding to the first ELIS is shown with italic and to the third ELIS with standard font) together with TrcR3 5′-AGACCGCTTCTGCGTTCTGA, which is complementary to the vector sequence downstream to IL-13 gene, and 13D2BR 5′-CAGGGCTGCACAGTA*TACCATGCT-GCCATTGCAG* together with ClaIF13 5′-CCACCAATC-GATATGGGTCCAGTTCCACCATC, which corresponds to the 5′ part of the IL-13 gene. The fragments containing overlapping regions at the site of the introduced deletion were amplified on pHIL13 matrix, purified from 1.5% agarose gel, and combined in the next PCR round with primers TrcR3 and ClaIF13. The PCR conditions were as follows: initial denaturation at 95°C for 3 min; 25 cycles (denaturation at 95°C for 45 sec, primer annealing at 52-55°C for 45 sec, elongation at 72°C for 1 min), final extension at 72°C for 5 min.

To obtain the fragments of the DV148 mutant gene, we used primers 13D3BF 5′-*TGACCGCTGGCATG*TGCC-CGCACAAGGTCTC (the part of the primer corresponding to the second ELIS is shown with italic and to the fourth ELIS with standard font) together with TrcR3 and the 13D3BR 5′-GACCTTGTGCGGGCA*CATGCCA-GCGGTCAGGTTG* and ClaIF13. SOE-PCR was conducted as described above for DV146.

The coding sequences for the deletion variants DV146 and DV148 were thus constructed. After cleavage by *Sac*I and *Hin*dIII and purification in 1.5% agarose gel, they were cloned to the vector pHIL13 treated with the same enzymes.

Protein expression and purification. *Escherichia coli* BL21(DE3) cells (Novagen, USA) were transformed by pHIL13, pDV156, or pDV148 plasmids and cultivated at 37°C in 200 ml of LB medium up to A_{560} 0.5-0.7. The cells were induced by addition of 0.5 mM isopropyl-β-D-thio-galactoside (IPTG) followed by 3-h incubation. Then cells were resuspended in buffer A (50 mM Tris-HCl, pH 8.0, 1 mM EDTA, 100 mM NaCl) and subjected to ultrasonic disintegration. The pellet was washed in buffer A containing 0.5% Triton X-100 and 2 M urea and dissolved in 2 ml of buffer B (20 mM Tris-HCl, pH 8.8, 0.4 M sodium sulfite, 0.15 M potassium tetrathionate,

6 M guanidinium chloride) for 16 h at room temperature with stirring. After centrifugation, the supernatant was diluted fourfold with buffer C (20 mM Tris-HCl, pH 8.0, 6 M guanidinium chloride, 10 mM imidazole) and transferred to a Ni-Sepharose (GE Healthcare, Sweden) column equilibrated with the same buffer. The column was washed with buffer D (20 mM Tris-HCl, pH 8.0, 8 M urea, 0.5 M NaCl, 20 mM imidazole), and the same buffer containing 300 mM imidazole was used for elution. The eluted protein was applied to a Sephadex G-100 column equilibrated with buffer E (20 mM Tris-HCl, pH 8.0, 8 M urea, 20 mM NaCl, 1 mM EDTA). The chromatography employed the same buffer at 2 ml/h rate. The protein purified by gel filtration was diluted to 100 μg/ml in renaturation buffer (20 mM Tris-HCl, pH 9.0, 1 M glycine, 1 mM EDTA, 0.1 M NaCl, 3 mM cysteine, 1.5 mM 2-mercaptoethanol), incubated at 4°C for 12 h, and dialyzed three times against 25 mM Na_2HPO_4, pH 8.0, 1 mM EDTA, 100 mM NaCl buffer. The protein preparations were concentrated in an Amicon cell on YM3 membrane whenever required.

Activity assay. The biological activity of IL-13 and its deletion variants was tested by stimulation of proliferation of TF-1 erythroleukemia cell line [18], which was obtained from the American Type Culture Collection (CRL-2003). Proliferation assays were performed as described previously [19]. Briefly, 15,000 TF-1 cells/well were cultured in 96-well plates in RPMI-1640 with 2% fetal bovine serum. Various concentrations of wild-type IL-13 or mutant DV148 or DV146 were added to the wells, and the cells were cultured for 5 days. Tritiated thymidine (1 μCi) was added to each well 18 h before the plates were harvested, and filter mats were counted in a RackBeta β-counter (LKB, Sweden).

RESULTS

Informational structure of IL-13. Informational structure of IL-13 (Fig. 1) is represented by three ELIS, separated by W34, Y43, and C70 residues, and one first-rank tree. The high-ranking ELIS are located in the N- and C-terminal regions of the IL-13 sequence. The fragment corresponding to the first-rank tree is flanked by the W34 and Y43 residues.

According to NMR spectroscopy data [8], IL-13 is a globular protein consisting of four α-helixes (A-D) connected with loops (Fig. 2a). Comparison of secondary structure and informational structure elements in IL-13 elucidates the following correlation: the first ELIS includes helix A, helixes B and C comprise the third ELIS, and helix D is a part of the fourth ELIS (Fig. 2b). Extended loops connecting helixes A with B and C with D are located in the second and fourth ELIS, correspondingly. It should be mentioned that this comparison is provided for illustrative purposes only; the ANIS

method is fully based on the primary sequence data and does not require any spatial structure information.

Construction of deletion variants. The artificial IL-13 deletion mutants were constructed by removal of regions corresponding to the individual elements of informational structure (Fig. 1, c and d). According to the data derived from point mutagenesis and IL-13/receptor complex simulation, residues of helixes A and D make the

a
```
GPVPPSTALR ELIEELVNIT QNQKAPLCNG SMVWSINLTA GMYCAALESL INVSGCSAIE KTQRMLSGFC
PHKVSAGQFS SLHVRDTKIE VAQFVKDLLL HLKKLFREGR FN
```
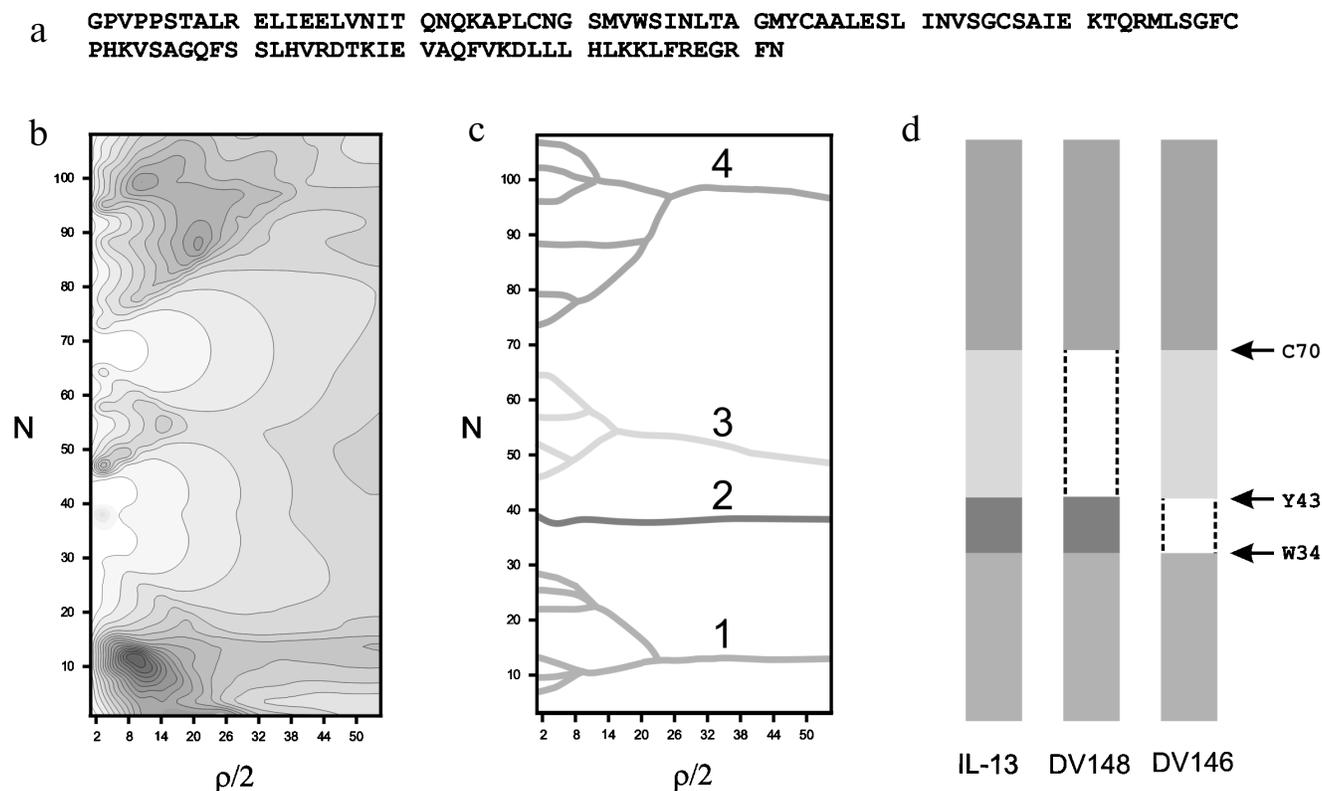
Fig. 1. Outline of IL-13 informational analysis. a) Amino acid sequence of human IL-13. b) Surface Γ_ω calculated using the ANIS method. c) IDIC-diagram of human IL-13. High-ranking ELIS (1-4) are depicted by different shades of gray. The axes in (b) and (c) are: horizontal, $\rho/2$ (site length/2), and vertical, N, amino acid residue position in the protein sequence. d) Ribbon diagrams of human IL-13 and its deletion variants. Arrows indicate residues (W34, Y43, and C70) corresponding to the boundaries between high-ranking ELIS.
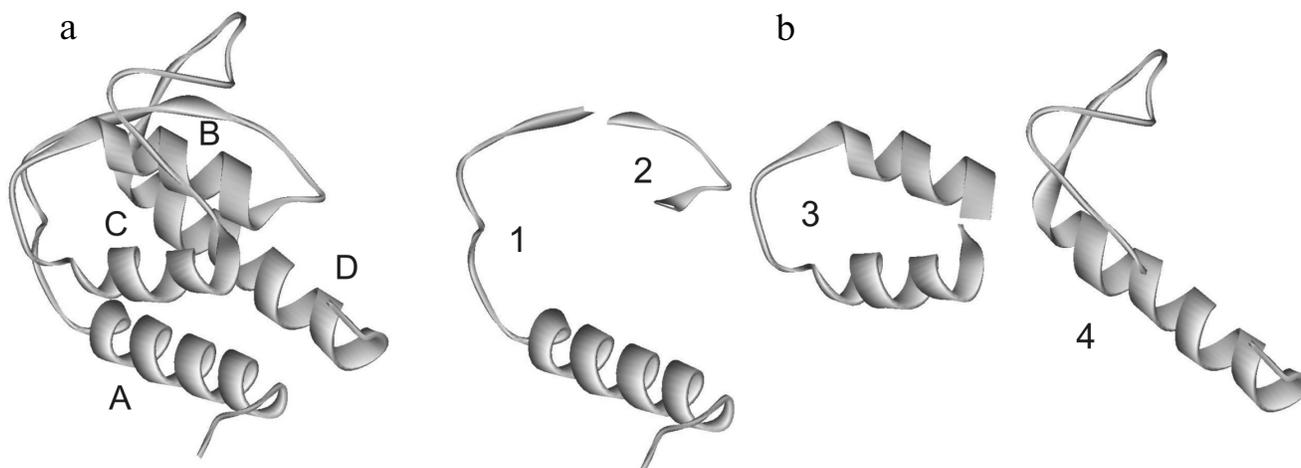
Fig. 2. a) The 3D structure of human IL-13 (1ijz.pdb). α-Helixes are designated A-D. b) Elements of IL-13 3D structure and corresponding high-ranking ELIS (1-4 as on Fig. 1c). ELIS 2 and 3 were deleted in DV146 and DV148, respectively.
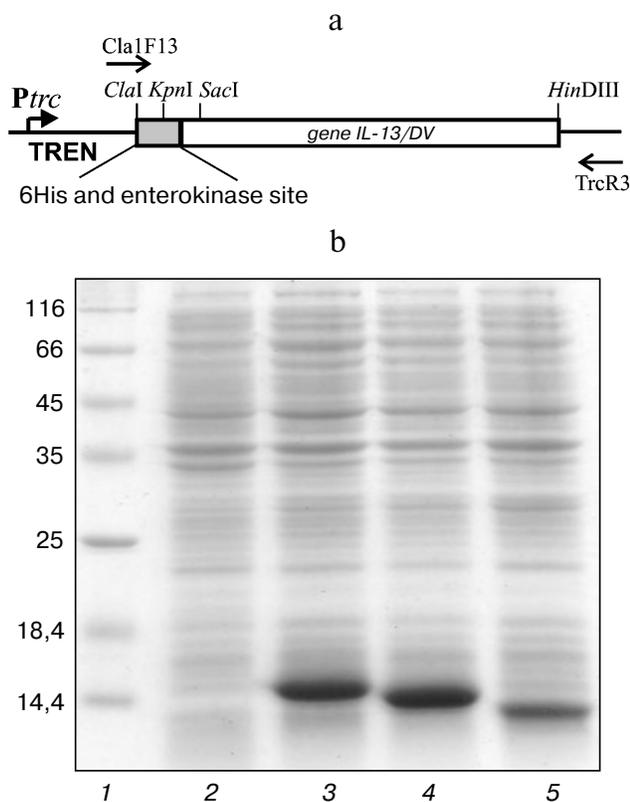
Fig. 3. a) Schematic diagram of human IL-13 and mutant DV146 and DV148 expression cassettes. The hexahistidine affinity tag and enterokinase cleavage site are in gray. TREN is the T7 bacteriophage gene *10* translation enhancer. The sites of annealing of primers TrcR3 and ClaIF13 are shown. b) SDS-PAGE analysis of BL21(DE3) cells without plasmid (*2*), transformed with pHIL13 (*3*), pDV146 (*4*), and pDV148 (*5*) after induction with IPTG. Lane *1*, molecular weight markers (Fermentas).

DV148 mutants match the expected values (13.0 and 11.2 kD, respectively).

After solubilization in denaturing conditions, the proteins were purified by metal chelating chromatography and gel filtration and then renatured by dilution in buffer containing redox reagents. The yield of the purification procedure is about 2-3 mg/liter.

Biological activity of IL-13 deletion variants. Biological activity of the preparations was tested by addition of titrated quantities of protein to the TF-1 cell line culture expressing heterodimeric IL-13/IL-4 receptor [22]. Previously obtained recombinant IL-13 was used as a control sample. The rate of proliferation stimulation was measured by ^{3}H-labeled thymidine incorporation. Maximal stimulation rate (1068%) is achieved by the addition of IL-13 to 300 ng/ml, whereas the dose necessary for 50% stimulation is 75 ng/ml (Fig. 4). The DV146 mutant lacks the ability to stimulate TF-1 cell proliferation in the studied range of dilutions (0.01-1000 ng/ml), while DV148 variant displays ~50% activity compared to the control sample. The dose of DV148 required for 50% stimulation is 160 ng/ml, which is 63% higher than in the case of the full-length protein.

According to the results, we studied DV146 antagonistic activity. The TF-1 cells were cultivated in the presence of full-length IL-13 (100 and 200 ng/ml) and different dilutions of the deletion variant. It was found that the addition of DV146 to 500 ng/ml concentration leads to suppression of IL-13 mitogenic activity, where the degree of suppression depends on DV146/IL-13 ratio. A 2.5-fold excess of DV146 inhibits 57% of IL-13 activity, while 5-fold excess suppresses up to 80% (Fig. 5).

principal contribution to such interaction [20, 21]. Since the novel deletion forms should posses an ability to bind the receptor, the primary structure regions responsible for formation of α-helixes A and D (i.e. N- and C-terminal ELIS) must remain unaltered.

We created the following deletion variants of IL-13: DV146 lacking fragment W35-M43 and DV148 lacking fragment Y44-F70. Such deletion boundaries correspond to the individual elements of IL-13 informational structure (Fig. 1d). We used the SOE-PCR method with a set of overlapping deletion primers and a pair of flanking primers to construct the genes of IL-13 deletion variants. The encoding sequences of IL-13 modified forms were cloned into pHIL13 plasmid (Fig. 3a) carrying full-length IL-13 gene under the control of the trc-promoter and TREN translation enhancer.

The SDS-PAGE analysis of pDV146/pDV148-transformed *E. coli* BL21(DE3) culture samples indicated that IPTG induction promotes efficient synthesis of IL-13 deletion variants in the form of inclusion bodies (Fig. 3b, lanes *3-5*). The electrophoretic mobilities of DV146/

Fig. 4. Proliferation of TF-1 cells induced by wild-type IL-13 and mutants DV148 and DV146.
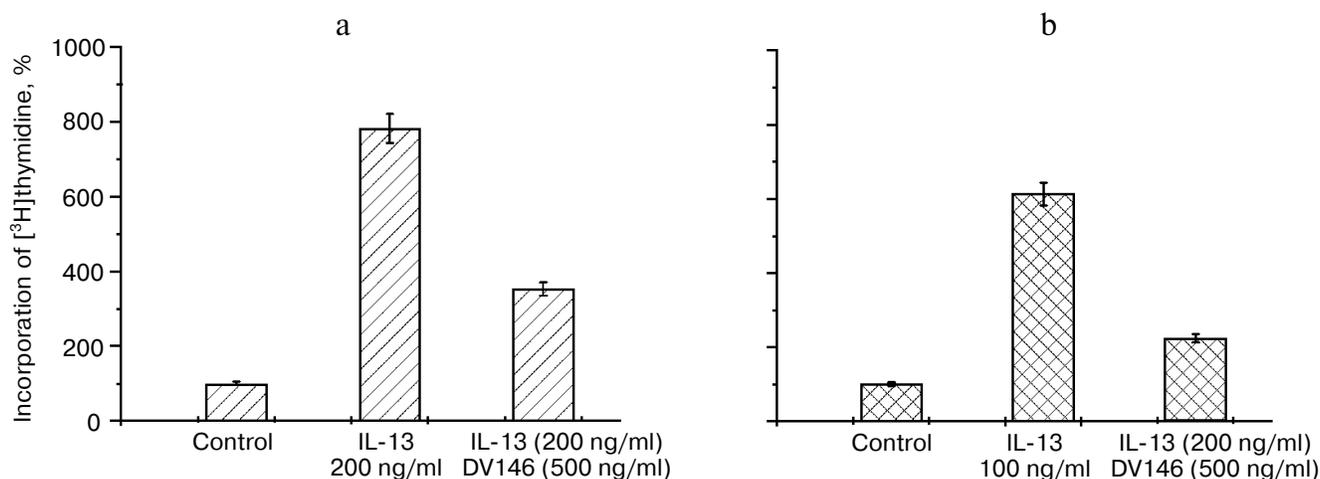
Fig. 5. Suppression of TF-1 cells proliferation induced by DV146. a) Cells were cultured in the presence of 200 ng/ml of IL-13 ± 500 ng/ml of DV146. b) Cells were cultured in the presence of 100 ng/ml of IL-13 ± 500 ng/ml of DV146.

DISCUSSION

The current manuscript describes design, cloning, and isolation of recombinant IL-13 deletion variants, which suppress TF-1 cell line proliferation induced by IL-13. The ANIS method was used to divide the amino acid sequence of IL-13 into fragments corresponding to high-ranking ELIS. We have shown previously that these structurally stable protein fragments could be removed without significant disturbances in protein folding [12].

The study of the biological activity of IL-13 deletion variants indicated that they differ in ability to stimulate the proliferation of TF-1 cell line. DV146 mutant (missing the W35-M43 region) completely lacks any ability to stimulate proliferation, while DV148 deletion form (Y44-F70 region removed) retains about 50% of full-length protein activity. The first deletion region (W35-M43), which is nine residues in length, is a part of a loop connecting the first and second α-helices in the cytokine molecule, whereas the second region (Y44-F70), 27 residues in length, includes the second and the third (partially) helixes [8]. The results provide evidence of the importance of the W35-M43 region for the interaction between IL-13 and its receptor, since the removal of the Y44-F70 region, which is three times longer, leads to a relatively small decrease in cytokine activity. Also, it is possible that the W35-M43 deletion may have caused the spatial structure alterations of the IL-13 molecule. However, we suppose that such modification should not affect protein structure in general, for it was shown that high-ranking ELIS are relatively independent and structurally stable elements [12, 23].

The mutagenesis of individual residues of IL-13 provides support for the fundamental impact of A and D helices in the association with the receptor [20, 21].

Mutations R66D and S69D targeting C helix residues lead to remarkable decrease in activity of the mutants, but this effect is not as pronounced as in the case of mutants E13K and R109D [20]. Thus, our results concerning 50% activity preservation of the Y44-F70 deletion variant are consistent with the point mutagenesis data.

We have determined that the simultaneous addition of full-length IL-13 and DV146 deletion variant to a TF-1 cell culture leads to decrease in proliferation rate, i.e. the mutant form manifests antagonistic behavior relative to the full-length protein. The mechanism of such effect is unknown; however, we speculate that the deletion slightly alters the protein surface in such a way that it still binds the receptor, but the signal transduction becomes impossible. Such a protein might be of use to counter the negative effects of IL-13 concentration increase, for example, in the case of asthma or other disorders of allergic nature.

According to our results, the ANIS method is an effective tool for protein structure and function study, and it can be applied to the design of truncated forms of native proteins, including receptor antagonists, by the removal of sequence fragments corresponding to predicted high-ranking ELIS.

REFERENCES

1. Minty, A., Chalon, P., Derocq, J. M., Dumont, X., Guillemot, J. C., Kaghad, M., Labit, C., Leplatois, P., Liauzun, P., and Miloux, B. (1993) *Nature*, **362**, 248-250.

2. McKenzie, A. N. J., Culpepper, J. A., Malefyt, R. D., Briere, F., Punnonen, J., Aversa, G., Sato, A., Dang, W., Cocks, B. G., and Menon, S. (1993) *Proc. Natl. Acad. Sci. USA*, **90**, 3735-3739.

3. Cosentino, G., Soprana, E., Thienes, C. P., Siccardi, A. G., Viale, G., and Vercelli, D. (1995) *J. Immunol.*, **155**, 3145-3151.

4. Mueller, T. D., Zhang, J. L., Sebald, W., and Duschl, A. (2002) *Biochim. Biophys. Acta*, **1592**, 237-250.

5. Punnonen, J., Aversa, G., Cocks, B. G., McKenzie, A. N., Menon, S., Zurawski, G., de Waal Malefyt, R., and de Vries, J. E. (1993) *Proc. Natl. Acad. Sci. USA*, **90**, 3730-3734.

6. Akdis, M., Akdis, C. A., Weigl, L., Disch, R., and Blaser, K. (1997) *J. Immnol.*, **159**, 4611-4619.

7. Wills-Karp, M., Luyimbazi, J., Xu, X., Schofield, B., Neben, T. Y., Karp, C. L., and Donaldson, D. D. (1998) *Science*, **282**, 2258-2261.

8. Moy, F. J., Diblasio, E., Wilhelm, J., and Powers, R. (2001) *J. Mol. Biol.*, **310**, 219-230.

9. Atamas, S. P., Choi, J., Yurovsky, V. V., and White, B. (1996) *J. Immunol.*, **156**, 435-441.

10. Tsytsikov, V. N., Yurovsky, V. V., Atamas, S. P., Aims, W. J., and White, B. (1996) *J. Biol. Chem.*, **271**, 23055-23060.

11. Nekrasov, A. N. (2004) *J. Biomol. Struct. Dyn.*, **21**, 615-624.

12. Nekrasov, A. N., Radchenko, V. V., Shuvaeva, T. M., Novoselov, V. I., Fesenko, E. E., and Lipkin, V. M. (2007) *J. Biomol. Struct. Dyn.*, **24**, 455-462.

13. Nekrasov, A. N. (2002) *J. Biomol. Struct. Dyn.*, **20**, 87-92.

14. Vriend, G. (1990) *J. Mol. Graph.*, **8**, 52-56.

15. Sambrook, J., and Russell, D. W. (2001) *Molecular Cloning: A Laboratory Manual*, Cold Spring Harbor Laboratory Press, Cold Spring Harbor, N. Y.

16. Shingarova, L. N., Kashyap, S. K., Petrovskaya, L. E., Petrenko, L. A., Pustoshilova, N. M., Sinichkina, S. A., and Korobko, V. G. (1998) *Biotekhnologiya*, **6**, 24-35.

17. Smirnov, D. V., Smirnova, M. G., Korobko, V. G., and Frolova, E. I. (1995) *Gene*, **155**, 277-281.

18. Kitamura, T., Tange, T., Terasawa, T., Chiba, S., Kuwaki, T., Miyagawa, K., Piao, Y. F., Miyazono, K., Urabe, A., and Takaku, F. (1989) *J. Cell Physiol.*, **140**, 323-334.

19. Oshima, Y., Joshi, B. H., and Puri, R. K. (2000) *J. Biol. Chem.*, **275**, 14375-14380.

20. Thompson, J. P., and Debinski, W. (1999) *J. Biol. Chem.*, **274**, 29944-29950.

21. Madhankumar, A. B., Mintz, A., and Debinski, W. (2002) *J. Biol. Chem.*, **277**, 43194-43205.

22. Obiri, N. I., Leland, P., Murata, T., Debinski, W., and Puri, R. K. (1997) *J. Immunol.*, **158**, 756-764.

23. Nekrasov, A. N., and Zinchenko, A. A. (2008) *J. Biomol. Struct. Dyn.*, **25**, 553-562.